Journal of Taibah University Medical Sciences (2024) 19(4), 753–765

Taibah University

Journal of Taibah University Medical Sciences

www.sciencedirect.com

Original Article

Zanthoxylum zanthoxyloides (Lam.) B. Zepernick & Timler alkaloidal extract exerts hepatoprotective effects in rats with a CCl_4/olive oil-induced hepatocellular carcinoma-like phenotype

Alex Boye, PhD [a,*], Victor A. Barku, PhD [b], Justice K. Addo, PhD [b], Orleans Martey, PhD [c], Ernest A. Asiamah, PhD [d], Mainprice A. Essuman, PhD [a] and Dennis Doe, PhD [a]

[a] *Department of Medical Laboratory Science, School of Allied Health Sciences, College of Health and Allied Sciences, University of Cape Coast, Cape Coast, Ghana*
[b] *Department of Chemistry, School of Physical Sciences, University of Cape Coast, Cape Coast, Ghana*
[c] *Department of Pharmacology, Center for Plant Medicine Research, Mampong-Akuapem, Ghana*
[d] *Department of Chemistry, School of Physical Sciences, College of Agriculture and Natural Sciences, University of Cape Coast, Ghana*

Received 4 March 2024; revised 8 May 2024; accepted 28 June 2024; Available online 10 July 2024

الملخص

أهداف البحث: قامت الدراسة بتقييم التأثير الوقائي المضاد لسرطان الكبد من المستخلص القلوي الجذعي والجذري المشترك لزانثوكسيلوم زانثوكسيلويدز في الفئران الشبيهة بسرطان الكبد سي سي آي 4 / المستحثة بزيت الزيتون.

طريقة البحث: تم تحضير المستخلص القلوي الجذعي والجذري المشترك لزانثوكسيلوم زانثوكسيلويدز من الساق المجففة وجذور زانثوكسيلوم زانثوكسيلويدز بنسبة 1:1 وتميزت كيميائيا. تم توزيع ما مجموعه 30 من فئران ويستار الذكور الأصحاء (يتراوح وزنها بين 210-280 جم) بشكل عشوائي على ست مجموعات (التحكم، والنموذج، و العلاج الكيمائي المستخدم لعلاج السرطان كابيسيتابين، وجرعات المستخلص القلوي الجذعي والجذري المشترك لزانثوكسيلوم زانثوكسيلويدز [50، 100، و200 ملغم/كغم]). تلقت جميعها، باستثناء المجموعة الضابطة، رباعي كلوريد الكربون/زيت الزيتون (3 مل/كجم، ص) في الصباح بينما في فترة ما بعد الظهر من نفس يوم الجرعة، تلقت المجموعة النموذجية محلول ملحي عادي (5 مل/كجم، ص)، ومجموعة كابيسيتابين (50 مجم/كجم). ومجموعات المستخلص القلوي الجذعي والجذري المشترك لزانثوكسيلوم زانثوكسيلويدز(50 ، و 100، و 200 ملغم / كغم) مرة واحدة في الأسبوع لمدة 36 يوما. تم رصد معدل البقاء على قيد الحياة، والبروتين ألفا في الدم والبروتين سي التفاعلي. تم تقييم تشريح الكبد الإجمالي، وأنسجة الكبد، وإنزيمات الكبد، البيليروبين، الكرياتينين، اليوريا، الألبومين، الجلوبيولين، والمعلمات الدموية.

النتائج: كان العائد من المستخلص القلوي الجذعي والجذري المشترك لزانثوكسيلوم زانثوكسيلويدز 0,58%. تم اكتشاف قلويدات الفينانثريدين الرباعية في المستخلص القلوي الجذعي والجذري المشترك لزانثوكسيلوم زانثوكسيلويدز. وكان معدل البقاء على قيد الحياة في فئران السيطرة 100٪ مقارنة مع الفئران في المجموعة النموذجية. أدى علاج المستخلص القلوي الجذعي والجذري المشترك لزانثوكسيلوم زانثوكسيلويدز إلى تحسين معدل البقاء على قيد الحياة مقارنة بالمجموعة النموذجية. زادت مستويات مصل والبروتين ألفا في الدم وبروتين سي التفاعلي والبيليروبين في المجموعة النموذجية مقارنة بالمجموعة الضابطة. انخفض المستخلص القلوي الجذعي والجذري المشترك لزانثوكسيلوم زانثوكسيلويدز في المصل والبروتين ألفا في الدم وبروتين سي التفاعلي والبيليروبين مقارنة بالنموذج. زاد مستوى انزيمات الكبد في المجموعة النموذجية مقارنة بالمجموعة الضابطة ولكن انخفض في المجموعة المعالجة بالمستخلص القلوي الجذعي والجذري المشترك لزانثوكسيلوم زانثوكسيلويدز.

الاستنتاجات: أظهر المستخلص القلوي الجذعي والجذري المشترك لزانثوكسيلوم زانثوكسيلويدز تأثيرا وقائيا مضادا لسرطان الكبد ضد الأنماط الظاهرية المشابهة لسرطان الكبد سي سي آي 4 / زيت الزيتون في الجرذان. يسلط هذا الاكتشاف الضوء على إمكانات القلويدات الخام من زانثوكسيلوم زانثوكسيلويدز كقوالب طبيعية للتوليف شبه العلاجي المضاد لسرطان الكبد.

الكلمات المفتاحية: ألفا-البروتين الجنيني؛ البروتين سي التفاعلي؛ رابع كلوريد الكربون؛ سرطان الكبد؛ قلويدات الفينانثريدين الرباعية؛ زانثوكسيلوم زانثوكسيلويدز

* Corresponding address: Department of Medical Laboratory Science, PMB UCC, Cape Coast, Ghana.
E-mail: aboye@ucc.edu.gh (A. Boye)

Peer review under responsibility of Taibah University.

ELSEVIER Production and hosting by Elsevier

 https://doi.org/10.1016/j.jtumed.2024.06.009

Abstract

Objective: This study assessed the prophylactic anti-HCC effects of a combined stem and root alkaloidal extract of *Zanthoxylum zanthoxyloides* (*Z. zanthoxyloides*) (SRAEZZ) in rats with a CCl_4/olive oil-induced HCC-like phenotype.

Methods: SRAEZZ was prepared from dried stems and roots of *Z. zanthoxyloides* in a 1:1 proportion and chemically characterized. A total of 30 healthy male Wistar rats (weighing 210–280 g) were randomly assigned to six groups (control, model, capecitabine, and SRAEZZ [50, 100, or 200 mg/kg]). All groups except the control received CCl_4/olive oil (3 mL/kg, *po*) in the morning, whereas in the afternoon of the same dosing day, the model group received normal saline (5 mL/kg, *po*), the capecitabine group received capecitabine (50 mg/kg, *po*), and the SRAEZZ groups received SRAEZZ (50, 100, or 200 mg/kg, *po*, respectively) once per week for 36 days. Survival rate, serum α-fetoprotein (AFP), and C-reactive protein (CRP) were monitored. Gross liver anatomy, liver histology, liver enzymes (ALP, AST, and ALT), bilirubin, creatinine, urea, albumin, globulins, and hematological parameters were assessed.

Results: SRAEZZ yield was 0.58% from the initial stem and root sample (520 g). Quaternary phenanthridin alkaloids were detected in SRAEZZ. Control rats had a 100% survival rate compared with rats in the model group. SRAEZZ treatment improved the survival rate with respect to that in the model group. Serum AFP, CRP, and bilirubin levels were greater in the model group than the control group. SRAEZZ decreased serum AFP, CRP, and bilirubin below the levels observed in the model group. ALP, AST, and AST were higher in the model group, but lower in SRAEZZ-treated group, than the control group.

Conclusion: SRAEZZ demonstrated prophylactic anti-HCC effects against CCl_4/olive oil-induced HCC-like phenotypes in rats. These findings highlight the potential of crude alkaloids from *Z. zanthoxyloides* as natural templates for semi-synthesis of anti-HCC pharmacotherapeutics.

Keywords: Alpha (α)-fetoprotein; C-reactive protein; Carbon tetrachloride; HCC; Quaternary phenanthridin alkaloids; *Z. zanthoxyloides*

Introduction

Cancer is a complex disease with many underlying etiologies whose main phenotypic hallmark is uncontrolled cell growth circumventing cell growth regulation. Globally, cancer afflicts millions of people. Primary liver cancer poses a major threat to global health.[1] Many histologic subtypes of primary liver cancer exist,[2] among which hepatocellular carcinoma (HCC) is the major histologic subtype.[3] HCC has the second highest incidence among all cancers and substantially contributes to cancer-related deaths globally.[4] As the major histologic subtype of primary liver cancer, HCC accounts for most liver cancer diagnoses and deaths.[2] With its high fatality ratio, HCC is the third most common cause of cancer-related deaths worldwide.[5] Although HCC incidence and burden have a poor global outlook, its regional distribution is skewed toward developing countries, primarily in sub-Saharan Africa and Asia.[6] This trend is attributed to the high incidence of hepatitis B and C viral infections in these regions, among other factors.[7] In addition, the high incidence of HCC in Africa and Asia has been linked to high alcohol intake,[8] non-alcoholic fatty liver disease,[9] and exposure to aflatoxin B1.[10] Despite the high HCC incidence and burden in Africa and Asia, treatment/management remain a major challenge, given the deficiencies associated with available conventional treatments, such as poor survival rates post-treatment for most treatment modalities; high recurrence rates after surgical sectioning; and serious adverse effects from chemotherapy and radiotherapy. Consequently, global interest has been renewed in the use of complementary and alternative medicines, primarily herbal medicines.[11] This shift has led to a corresponding increase in natural product research aimed at exploring global biodiversity hotspots for natural products, specifically medicinal plants with potential anti-cancer properties.[12] This paradigm has received some form of endorsement from the World Health Organization,[13] which recommends that natural product-inspired drugs be subjected to thorough scientific scrutiny and validation, just like their conventional counterparts, to ensure safety and efficacy.

Medicinal plants in the genus *Zanthoxylum* have recently become a focus of natural product research, because of evidence suggesting that they might contain anti-cancer secondary plant metabolites.[14] For example, crude alkaloidal extract from the leaves of *Z. zanthoxyloides* has shown anti-HCC effects *in vivo*.[15] Chelerythrine, an isoquinolone alkaloid isolated from the roots of *Zanthoxylum asiaticum*, has demonstrated anti-cancer properties against several cancer subtypes,[16] and the mechanism of its anti-cancer properties has been found to be associated with modulation of many signaling pathways implicated in cancer, including DNA interaction.[17]

Curative anti-HCC effects of alkaloidal leaf extract of *Z. zanthoxyloides* have been demonstrated in rats with a CCl_4/olive oil-induced HCC-like phenotype.[15] However, the alkaloid bio-distribution in other parts of *Z. zanthoxyloides* and their possible anti-HCC effects, particularly prophylactic anti-HCC effects, remain unknown. This study therefore assessed the prophylactic anti-HCC effects of combined stem and root alkaloidal extract of *Z. zanthoxyloides* (SRAEZZ) in a rat model of HCC induced by CCl_4/olive oil. In addition, chemical characterization of SRAEZZ was conducted to identify specific alkaloids potentially associated with the anti-HCC effects. Interestingly, SRAEZZ demonstrated

prophylactic anti-HCC effects in rats with an HCC-like phenotype, and two quaternary alkaloids (Q1 and Q2) were isolated from SRAEZZ.

Materials and Methods

Chemicals and drugs

Chemicals and reagents used in this study were of analytical grade, and included capecitabine, carbon tetrachloride, 70% ethanol, chloroform, ammonium hydroxide, hydrochloric acid (Thermo Fisher Scientific, Massachusetts, USA), and olive oil (AddPharma Ghana Limited, Accra, Ghana).

Preparation of stem and root alkaloidal extract of Z. zanthoxyloides

Alkaloid extraction was performed as previously described[15] with slight modifications. Briefly, dry pulverized stem and root samples of *Z. zanthoxyloides* (520 g) were extracted through cold maceration with 70% EtOH (v/v; 2 L) for 72 h. The crude ethanol extract was filtered and concentrated with a rotary evaporator (Eyela Co. Ltd, Tokyo, Japan). The process was repeated three times for optimization of the resultant crude ethanol extract. The crude ethanol extract was adjusted to pH 10 by addition of 25% NH_4OH (5 mL). To obtain SRAEZZ, we extracted the alkaloid component of the crude ethanol extract with chloroform ($CHCl_3$, v/v; 250 mL × 6) with a separating funnel. The $CHCl_3$ was evaporated to dryness to obtain SRAEZZ of mass 3.028 g. The entire extraction process was repeated several times to obtain a sufficient mass of SRAEZZ for all experiments. The alkaline aqueous layer was then acidified with concentrated HCl to pH 2. A saturated potassium iodide solution was prepared and added to the acidic solution. The iodide salts of quaternary alkaloidal bases were extracted with chloroform. The extraction with chloroform was repeated three times, each with 10 mL solvent. The combined chloroform extract containing the iodide salts of quaternary alkaloidal bases was concentrated to dryness, thus yielding 0.095 g. Hydrogen sulfide gas was bubbled through the mixture of iodide salts of quaternary alkaloidal bases to free the quaternary alkaloids. The mixture of crude alkaloids (0.052 g) was separated on an A12 03 column on a neutral and reanal activity grade II with chloroform as the eluting solvent, followed by other solvent systems; chloroform/methanol and methanol (10 mL fractions) served as eluents. This process was repeated several times with fresh crude alkaloid mixture from SRAEZZ. Two alkaloids were obtained from the combined fractions 56–92 (labeled QI) and fractions 98–134 (labeled Q2) after evaporation of the solvent and were purified by recrystallization from methanol. The masses obtained for Q1 and Q2 were 21 mg and 10 mg, respectively (Figure 1). The isolated compound Q2 was found to contain impurities, whereas the isolated compound Q1 was relatively pure.

Test for alkaloids

Both crude ethanol extract and SRAEZZ were tested for the presence of alkaloids with a previously described method.[18] Briefly, crude ethanol extract and SRAEZZ (5 mL each) were separately evaporated to dryness and basified by the addition of 25% NH_4OH (1 mL). Each mixture was poured into a separating funnel and extracted with chloroform ($CHCl_3$) (2 mL). The $CHCl_3$ fraction was evaporated to dryness and acidified with 2 M HCl added dropwise. Drops of Mayer's reagent were added to each mixture. The appearance of a creamy precipitate was indicative of the presence of alkaloids.

Chemical characterization of SRAEZZ

Compound analysis was not performed on SRAEZZ, because its impure alkaloidal nature did not permit spectral analysis. In addition, structural elucidation of compound Q2 was not performed because Q2 was impure (Figure 1). The structural identification of the isolated compound Q1 was performed with high resolution mass spectroscopy. The high resolution mass spectrum of the isolated compound Q1 was used to confirm its chemical structure, and indicated molecular ion $[M]^+$ and $[M + H]^+$ peaks at m/z 348 and 349, respectively. The molecular ion peak was also observed as a characteristic base peak of the compound at m/z 348. A methyl adduct of the $[M + H]^+$ peak comprising $[M + H + CH_3]^+$ was observed at m/z 364 (S1 and S2). Other prominent peaks confirming the structure of the isolated compound Q1 were observed in the fragmentation pattern at m/z 333, 318, 304, 290, and 275 (Figures 2 and S3).

Animal acquisition and husbandry

Healthy adult male Wistar rats (weighing 210–280 g) were purchased from the Animal Experimentation Unit, Department of Pharmacology and Toxicology, Center for Plant Medicine Research, Mampong-Akuapim, and maintained in cages at the animal house of the Center until use. The rats were kept under ambient conditions of temperature, humidity, atmospheric pressure, and a 12-h light–dark cycle. Unrestricted access to standard pelleted chow (Agricare Ltd, Kumasi) and sterilized distilled water was provided unless otherwise necessary to meet the specific requirements of some experiments.

Dose selection and bodyweight measurements

The selection of doses for the study was based on a previous study[15] and trial studies. After random assignment of rats into the various groups, the bodyweights of rats in each group were measured and referred to as day 0 bodyweights. Subsequently, bodyweight measurements were performed every week to enable adjustment of doses to reflect bodyweight changes. Bodyweights of surviving rats in each

group were measured on the final day of experimentation, just before the rats were sacrificed under deep anesthesia.

Animal groupings and experimental design

A total of 30 healthy adult male Wistar rats were randomly assigned into six groups of five rats each. The rats acclimated to laboratory conditions for 1 week before the commencement of experiments. Group 1 served as a control (receiving normal saline [5 mL/kg, *po*] in the morning and the afternoon) once per week; group 2 served as the model group (receiving CCl_4/olive oil [3 mL/kg *po*] in the morning and normal saline [5 mL/kg, *po*] in the afternoon) once per week; group 3 served as the standard (receiving CCl_4/olive oil [3 mL/kg, *po*] in the morning and capecitabine [10 mg/kg, *po*] in the afternoon) once per week; and groups 4, 5, and 6 received CCl_4/olive oil (3 mL/kg, *po*) in the morning and SRAEZZ (50, 100, and 200 mg/kg, *po*, respectively) in the afternoon once per week. The schedule of induction and treatment is described in S1.

Blood collection, liver perfusion, and isolation of organs

At the end of the experimental period, the rats were anaesthetized with ketamine (90 mg/kg, *ip*) and heparin (100 IU/mL *ip*). The livers were isolated and cannulated through a surgical technique as previously described.[19] Briefly, the liver was exposed through a midline incision. The common bile duct, the splenic and gastroduodenal veins, and the infra-renal and supra-celiac aortas were isolated and ligated. The supra-hepatic vena cava was cut off after incision of the diaphragm. Before washout, venous blood from the supra-hepatic vein was collected into sample tubes for biochemical assessments. The portal vein was isolated and cannulated (BD Insyte-W®, 16G, Le Point-de-Claix, France). The liver was washed out with Krebs's Henseleit physiological solution (20 mL) for 5 min through the portal vein, then subjected to formalin fixation and histological assessments.

Histological assessments

Histological sections were created by through a previously described method with slight modifications.[20] In brief, paraffin sections of buffered formalin-fixed liver tissues were dehydrated through three alcohol changes and xylenated. Semi-serial sections (5 μm) were created with a microtome (microtome HM-355S Automatic Microtomes, ermo-Scientific), then stained with Harris Hematoxylin and Eosin (H&E), mounted permanently on glass slides with distyrene plasticizer and xylene (DPX), placed under coverslips, and viewed under an optical microscope (Zeiss, Germany) coupled to a high-resolution camera (AmScope, California).

Measurement of biochemical parameters

For each batch of samples for each biochemical parameter, two assayed control materials were analyzed and run with each new calibration of the chemistry analyzer as well as each new reagent cartridge. All biochemical parameters (creatinine, urea, creatinine kinase-MB, creatinine kinase, C-reactive protein [CRP], α-fetoprotein [AFP], total protein, direct bilirubin, indirect bilirubin, total bilirubin, ALT, ALP, AST, GGT, and LDH) were monitored with a Mindray 480 chemistry analyzer (Shenzhen Mindray Bio-Medical Electronics Co., Ltd). Briefly, the chemistry analyzer was turned on and connected to Mindray operating software. The main interface program was selected, and the sample icon was clicked. Sample ID, position, and type were selected. From the chemistry parameter display, the parameter of interest was selected and saved. Each sample was loaded in the corresponding position in the sample carousel of the chemistry analyzer. The play display was clicked to run each sample. The chemistry analyzer automatically calculated the analyte concentration. After completion of the analysis, the results icon was clicked to display the results.

Measurement of electrolytes and hematological parameters

Serum electrolytes were measured with a Smartlyte Plus electrolyte analyzer (Diamond Diagnostic Inc.). Briefly, the home button was pressed to select the sample type. The door was opened when the analyzer displayed [OPEN DOOR]. Samples were introduced only when the analyzer displayed [LOAD SAMPLE], by moving the sample container to the sample probe, while ensuring that the probe opening was immersed in solution. Samples were removed when [WIPE PROBE & CLOSE DOOR] was displayed, and the sample door was closed.

HepG2 cell culture

Frozen HepG2 cell lines (American Type Culture Collection, Manassas, VA, USA) were obtained as a gift from Dr. Lily Paemka, WACCBIP, University of Ghana, Ghana. HepG2 cells were recovered, passaged several times, and grown as sub-confluent monolayer cultures in Dulbecco's modified Eagle's medium supplemented with 10% fetal bovine serum. Cells were maintained in 95% air and 5% CO_2 at 37 °C. Experiments were performed in the log-phase of growth 24 h after cells had been plated.

Trypan blue assays

Trypan blue assays were conducted to assess cell viability as previously described.[21] Briefly, HepG2 cell suspensions were centrifuged at $100\times g$ for 5 min. The supernatants were decanted and discarded. The cell pellets were re-suspended in serum-free complete medium (1 mL). The re-suspended cells (10 μL) were mixed with 0.4% trypan blue, then incubated in a microtiter plate for 3 min at room temperature. A drop of trypan blue/cell mixture was applied to a hemocytometer. The hemocytometer was placed on the stage of a binocular microscope (Zeiss, Germany) for counting of dead (blue-stained cells) and live (unstained cells) cells separately. To obtain the total number of dead and live cells per 1 mL aliquot of cell suspension, we multiplied each respective count by the dilution factor of the trypan blue.

Statistical analysis

Data for all measured endpoints (parameters) are expressed as means ± SD, n = 5. GraphPad Prism version 9 was used for statistical analysis and generating output graphs. Statistically significant differences between computed means of each parameter (endpoint) for the groups (control, model, capecitabine, and SRAEZZ) were established with one-way ANOVA with a 95% confidence interval and $p \leq 0.05$ considered significant (designated as $^{\#}$ control vs model; * model vs treatments, i.e., capecitabine and SRAEZZ); a post-hoc least-significant-difference test was subsequently performed.

Results

Yield of SRAEZZ

The yield of SRAEZZ was 0.58% (w/w). Two alkaloids were obtained from the combined fractions 56–92 (labeled QI) and fractions 98–134 (labeled Q2) after evaporation of the solvent, and were purified by recrystallization from methanol. The masses obtained for Q1 and Q2 were 21 mg and 10 mg, respectively. The isolated Q2 contained impurities, whereas Q1 was relatively pure (Figure 2, S2–S4).

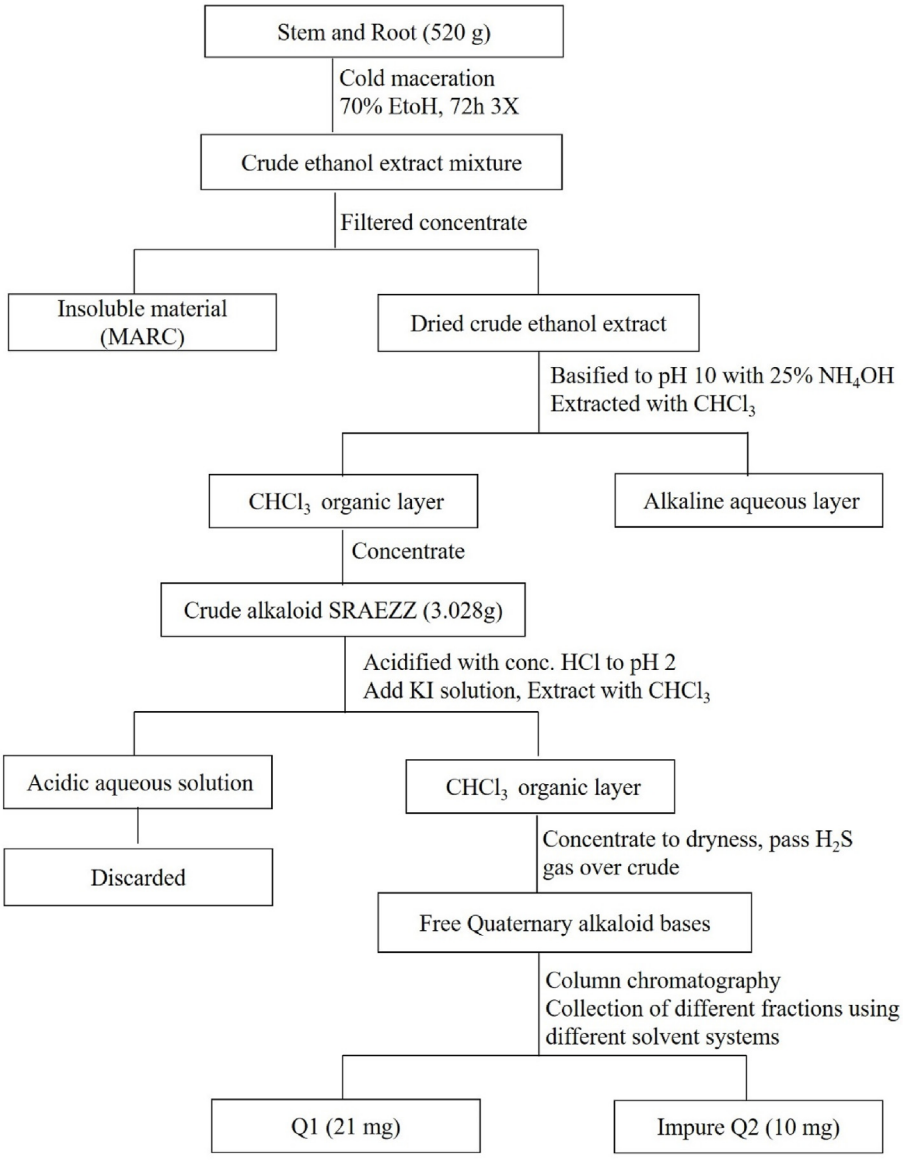

Figure 1: Flowchart showing the extraction of SRAEZZ and the isolated quaternary alkaloids (Q1 and Q2). SRAEZZ: Stem and root alkaloidal extract of *Z. zanthoxyloides*.

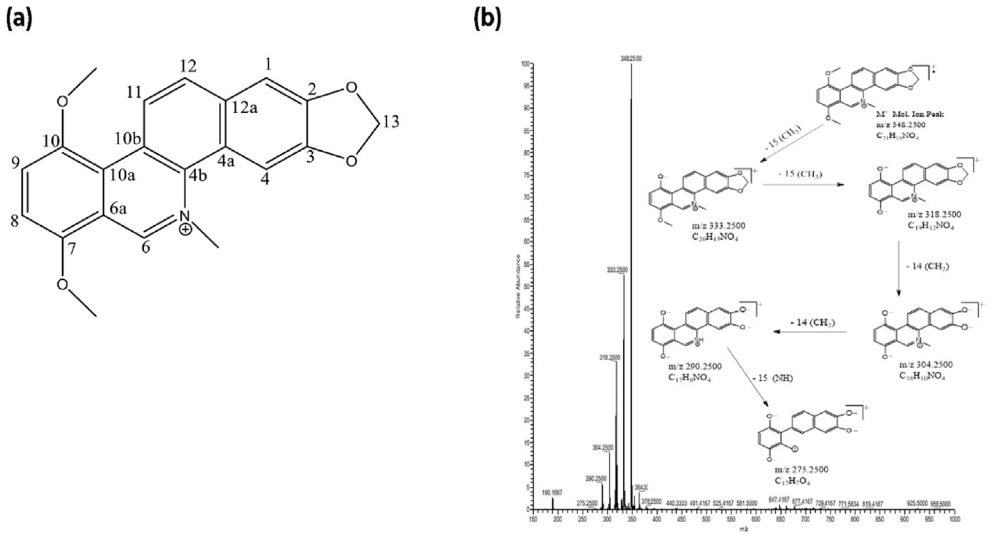

Figure 2: The chemical structure of the isolated quaternary alkaloid Q1 (1,4: dimethoxy-12-methyl-[1,3] dioxolo [4′,5′,5] benzo[1,2,-c] phenanthridin-12-ium); ESI−MS (positive mode) *m*/*z* 348[M^+] (a) and its fragmentation pattern (b).

Effects of SRAEZZ on α-fetoprotein and C-reactive protein

Serum levels of AFP were significantly greater in the model group than the control group. However, SRAEZZ and capecitabine treatments resulted in significantly lower serum AFP than observed in the model group. Notably, SRAEZZ led to a dose-dependent decrease in serum AFP (Figure 3A). Serum levels of CRP were lower in the control group than the model group. However, SRAEZZ and capecitabine treatments marginally decreased CRP below that observed in the model group (Figure 3B).

Effects of SRAEZZ on liver enzymes

In the control group, except for serum globulin, total bilirubin, serum LDH, direct bilirubin, serum total protein, serum albumin, and indirect bilirubin, which were marginally higher than observed in the model group, all other examined liver function enzymes, such as serum ALP, serum gamma-GT, serum ALT, and serum AST, were marginally lower than those in the model group. SRAEZZ and capecitabine treatments resulted in marginally lower serum gamma-GT, serum ALP, and serum ALT, but higher serum globulin, indirect bilirubin, direct bilirubin, and serum LDH, than observed in the model group (Figure 4).

Effects of SRAEZZ on liver histology

Control livers appeared normal, with no traces of any pathological features (Figure 5A). In contrast, the model livers showed visible diffuse tumor growth and a general rough appearance. However, SRAEZZ treated livers,

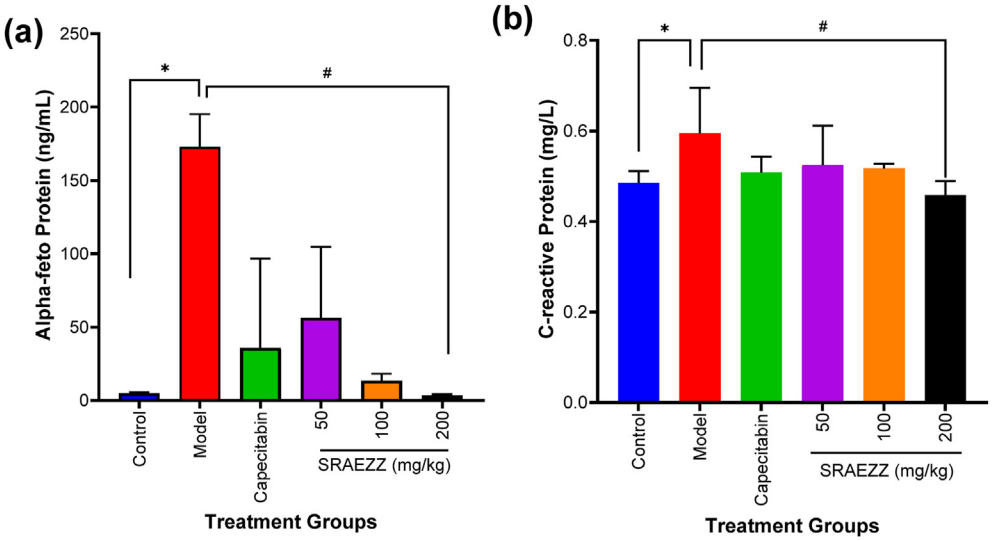

Figure 3: Cumulative effects of treatments on alpha (α)-fetoprotein (a) and C-reactive protein (b) over the entire treatment period. Each bar indicates mean ± SD, n = 5. *P ≤ 0.05 (control vs model); #P ≤ 0.05 (model vs treatments). SRAEZZ: Stem and root alkaloidal extract of *Z. zanthoxyloides*.

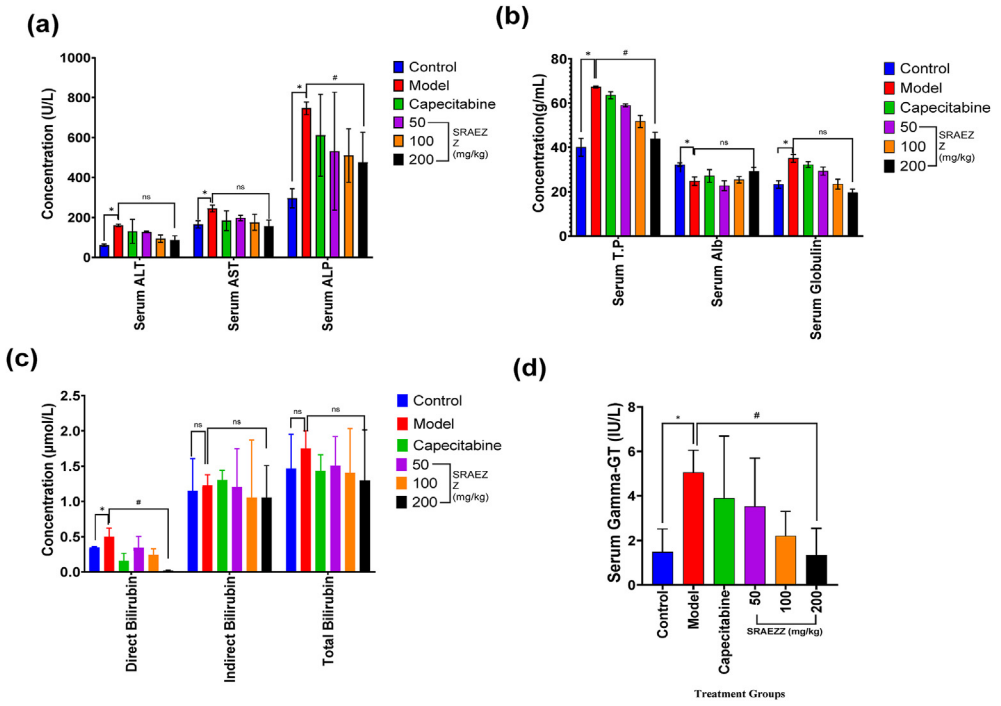

Figure 4: Cumulative effects of treatments on serum ALT, AST, and ALP (a), serum total protein, albumin, and globulin (b), serum direct bilirubin, indirect bilirubin, and total bilirubin (c), and serum gammaglutaryl phosphate (d) over the entire treatment period. Each bar indicates mean ± SD, n = 5. *P ≤ 0.05 (control vs model); #P ≤ 0.05 (model vs treatments). SRAEZZ: Stem and root alkaloidal extract of *Z. zanthoxyloides*.

compared with those in the model group, demonstrated improved liver gross anatomy. The histological sections of livers from model rats demonstrated nuclear crowding, pyknotic nuclei, fat accumulation, centrilobular necrosis, and severe mononuclear cell infiltration in the portal triad region and liver parenchyma, in contrast to observations in the control group. Compared with the model group, the SRAEZZ and capecitabine groups showed generally improved liver micro-histological structure (Figure 5B).

Effects of SRAEZZ on bodyweight, survival, and organ/bodyweight ratio

Bodyweights of rats were measured on days 1 and 36. In contrast to those in the control group, the rats in the model group had no weight gain but showed significant weight loss. Compared with rats in the model group, rats in the SRAEZZ and capecitabine groups showed weight gain, particularly those in the SRAEZZ (100 mg/kg) group. No mortality was observed among control rats, whereas more than half the rats in the model group died. Compared with that in the model group, survival was improved among the SRAEZZ and the capecitabine groups, particularly in the SRAEZZ (50 and 100 mg/kg) groups. The organ (liver, lungs, heart, kidney, and pancreas) weights of rats in the model group were marginally greater than those in the control group. Except for the lungs, the organ weights were lower in rats in the SRAEZZ and capecitabine groups than the model group. The liver/bodyweight ratio was greater in the model group than the control group. The liver/bodyweight ratio in the SRAEZZ and capecitabine groups was marginally lower than that in the model group, but the mean differences were insignificant (Figure 6).

Effects of SRAEZZ on kidney function

Given the direct relationship between renal and hepatic function, particularly in metabolism and the elimination of metabolites, we assessed how the treatments affected kidney function. Serum creatinine and urea levels were greater in the model group than the control group. The measured electrolytes were marginally greater in the control group than the model group. Serum chloride was comparable across all groups. SRAEZZ and capecitabine treatments led to marginally lower serum creatinine and urea levels than observed in the model group (Figure 7).

Effects of SRAEZZ on hematological parameters

In the model group, the monocyte, neutrophil, WBC, and eosinophil counts were greater, whereas the platelet and lymphocyte counts were marginally lower, than those in the control group (Figure 8). The other hematological parameters were comparable across all groups (S2).

Effects of SRAEZZ on HepG2 cells

To assess the cytotoxic effects of SRAEZZ, we used the humanized hepatoma cell line HepG2. SRAEZZ demonstrated concentration-dependent cytotoxicity against HepG2

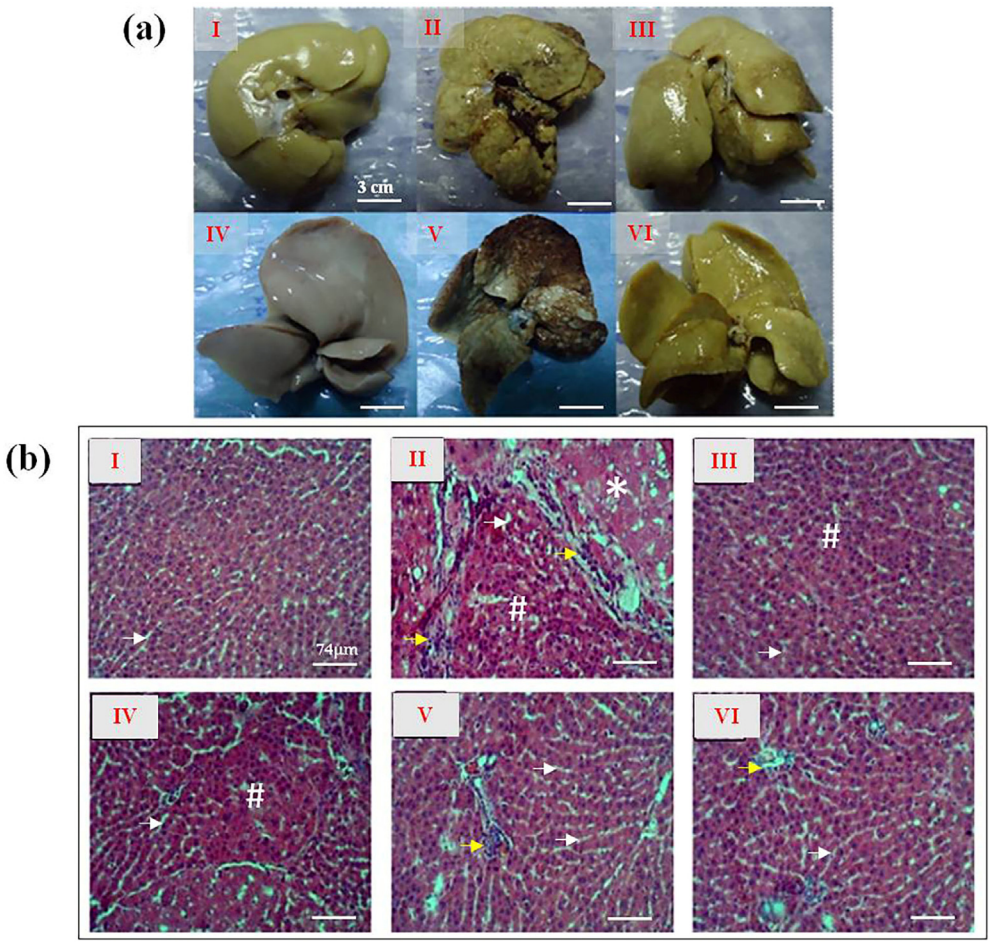

Figure 5: Effects of SRAEZZ and other treatments on the gross anatomy of liver tissues of rats with a CCl_4/olive oil-induced HCC-like phenotype (a), showing control (I), model (II) and SRAEZZ (100 mg/kg) (III); and histoarchitecture of H&E stained sections of representative livers (b). Control (A), model (B), capecitabine (C), SRAEZZ (50 mg/kg) (D), SRAEZZ (100 mg/kg) (E), and SRAEZZ (200 mg/kg) (F). Yellow arrow represents central vein; white arrow and * represent portal triad region; # represents sinusoids.

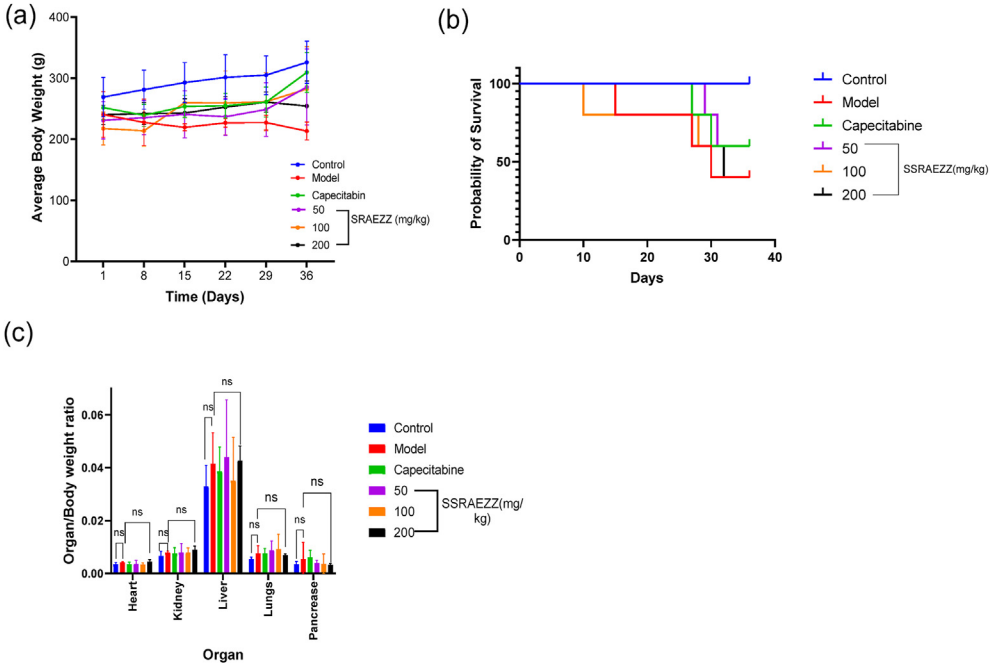

Figure 6: Effects of SRAEZZ on (a) bodyweight, (b) survival, and (c) organ/bodyweight ratio. ns: not significant; SRAEZZ: Stem and root alkaloidal extract of *Z. zanthoxyloides*.

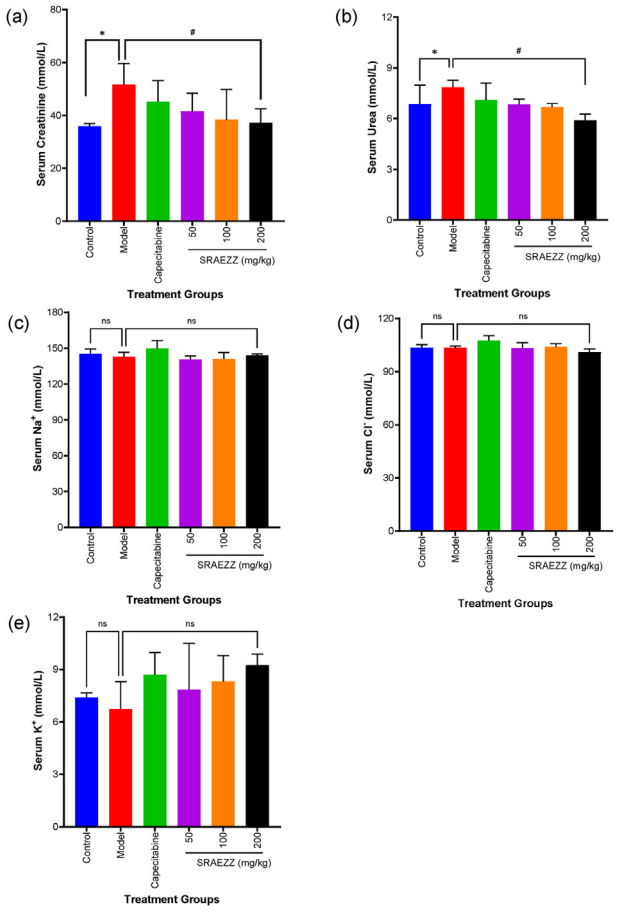

Figure 7: Cumulative effects of treatments on serum creatinine (a), serum urea (b), serum Na^+ (c), serum Cl^- (d), and serum K^+ (e) over the entire treatment period. Each bar indicates mean ± SD, n = 5. *P ≤ 0.05 (control vs model); #P ≤ 0.05 (model vs treatments). SRAEZZ: Stem and root alkaloidal extract of *Z. zanthoxyloides*.

cells, and this effect was comparable to that of capecitabine, except that capecitabine was more potent than SRAEZZ according to the IC_{50} estimates (S5).

Discussion

This study demonstrated the presence of quaternary phenanthridin alkaloids in SRAEZZ and prophylactic anti-HCC-like effects of SRAEZZ in rats with a CCl_4/olive oil-induced HCC-like phenotype. This finding corroborates those from a previous report indicating that crude alkaloidal extract from the leaves of *Z. zanthoxyloides* have curative anti-HCC effects.[15] Chemical hepatocarcinogenesis is induced in experimental animals primarily through use of liver-specific carcinogens, such as CCl_4 or diethylnitrosamine (DEN), thus providing valid models for testing the efficacy of investigational drugs. In this study, CCl_4 was used as a hepatocarcinogenic agent to induce HCC-like phenotypes in rats. Indeed, many studies have used CCl_4 as a fibrogenic or a carcinogenic agent in animal models of liver fibrosis and HCC, respectively.[22,23] The mechanism of CCl_4-induced HCC in rats involves initial enzymatic conversion of CCl_4 by hepatic cytochrome P450

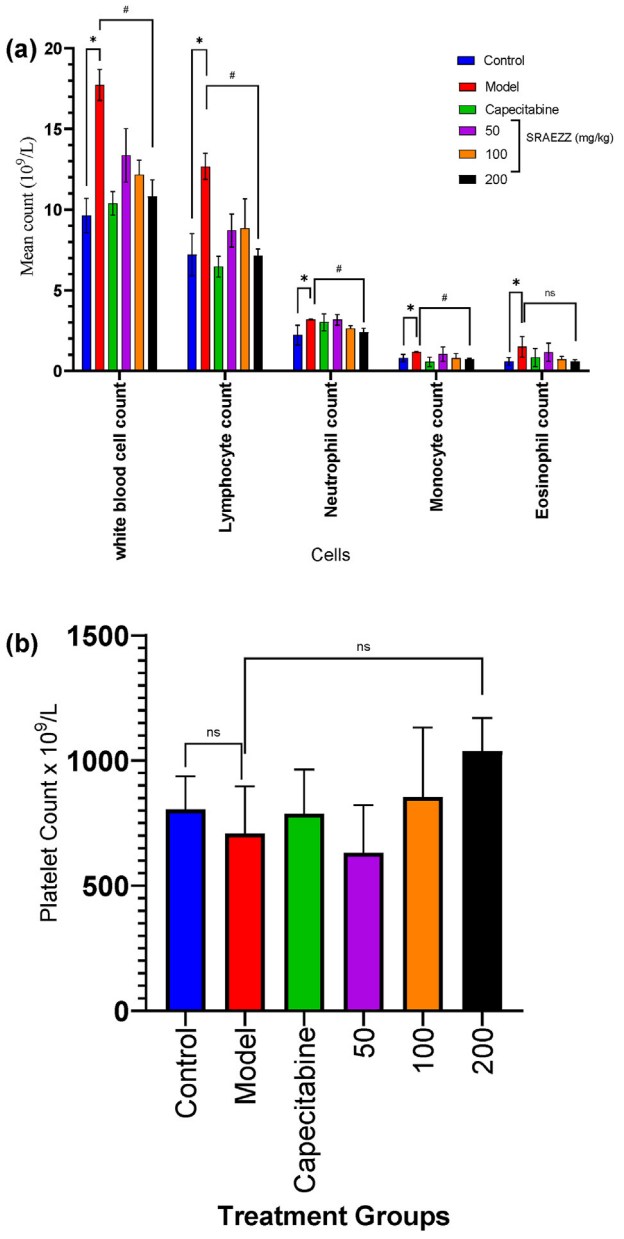

Figure 8: Cumulative effects of treatments on WBC count, lymphocyte count, neutrophil count, monocyte count, and eosinophil count (a) and platelet count (b) over the entire treatment period. Each bar indicates mean ± SD, n = 5. *P ≤ 0.05 (control vs model); #P ≤ 0.05 (model vs treatments). SRAEZZ: Stem and root alkaloidal extract of *Z. zanthoxyloides*; ns: not significant.

isoenzymes, specifically CYP2E1, into unstable chemical intermediates, such as trichloromethyl peroxyl radical (CCl_3OO^-), which chemically converts membrane bound unsaturated fatty acids into more potent endogenous radicals, such as lipid peroxyl radical, lipid alkoxyl radical, and 4-hydroxynon-2-enal.[24] These endogenously derived radicals from CCl_4 induce oxidative stress, lipid peroxidation, and DNA damage in hepatocytes and other hepatic cells.[24–26] Consequently, the structure and function of the liver become impaired, thus manifesting morphological changes in the hepatic microarchitecture, such as hepatocyte

necrosis, collapse of the portal triad, centrilobular necrosis, ballooning of hepatocytes, fat deposition, inflammatory cell infiltration, hepatocyte regeneration, and tumor growth.[24,27] Therefore, the CCl_4-induced HCC model presents an experimental HCC phenotype suitable for assessment of the efficacy and response of experimental animals to treatment. This study used a prophylactic HCC model, which enabled both HCC induction in rats and treatment with SRAEZZ and capecitabine concurrently at least 6 h apart. Survival rate, bodyweight changes, organ/bodyweight ratios, liver biosynthetic function (synthesis of proteins and enzymes by the liver, e.g., albumin and globulins), liver metabolism and detoxification function (e.g., metabolism of bilirubin), liver inflammation (CRP), hepatocyte regeneration (e.g., AFP), and liver histology (gross liver anatomy and liver histology) were monitored as endpoints to assess HCC burden and response to treatment.

AFP, an oncofetal-protein produced in abundance by fetal liver cells, has a key role in the transport of nutrients and other important biological molecules between the fetal and maternal circulations. After birth, AFP levels gradually decline in the sera of the mother and fetus, particularly during fetal growth. However, chemical-mediated hepatocyte injury confers AFP production ability on spontaneously regenerated hepatocytes often marked by elevated serum AFP. Thus, AFP is frequently used as a biomarker together with other assessments to diagnose HCC and other cancers.[28] Elevated serum levels of AFP were often observed in the model rats, because CCl_4 metabolic intermediates induce DNA damage in hepatocytes, thus restoring AFP production ability. We observed a significant decrease in serum AFP levels in SRAEZZ-treated rats with an HCC-like phenotype, thereby suggesting that SRAEZZ not only aided in recovery of necrotized hepatocytes but also restored normal hepatocyte function. Moreover, SRAEZZ decreased serum CRP levels, which were elevated together with AFP in model rats. Because CRP, an acute phase inflammatory biomarker, decreased in SRAEZZ-treated rats with an HCC-like phenotype, SRAEZZ may have anti-inflammatory properties and is worthy of further exploration as an adjunctive therapy against inflammation-associated cancers such as HCC.

The biosynthetic function of the liver is determined by the ability of the liver to biosynthesize several proteins, primarily transport proteins, such as albumin, globulins, and other proteins that play key roles in hemostasis including prothrombin.[29] In normal livers, the levels of these proteins are maintained within physiological limits to enable normal function. However, when the hepatic system is exposed to intense and chronic inflammation, as in the case of systemic CCl_4 exposure, gradual deterioration of liver function is observed, marked by elevation of specific liver enzymes. In the present study, model rats, in which HCC was chemically induced, without treatment, demonstrated significantly low levels of albumin and globulins, thus indirectly indicating the extensive destruction of hepatocytes by metabolic intermediates of CCl_4. The group with SRAEZZ treatment showed improvements in the ability of the liver to biosynthesize albumin and globulins, as compared with the observations regarding compromised liver biosynthetic function in the model rats. Inasmuch as compromised biosynthetic function of the liver relates directly to extensive destruction of hepatocytes by CCl_4 metabolic intermediates, the recovery of biosynthetic function, as observed in STRAEZZ treated rats with an HCC-like phenotype, emphasized the ability of SRAEZZ to antagonize the chemical reactivity of CCl_4 intermediates. Although many biomarkers enable direct/indirect diagnosis of the metabolic function of the liver, bilirubin is among the most frequently used biomarkers for assessing the metabolic and detoxifying capacity of the liver.

Under chronic inflammatory conditions, sudden elevations in the levels of some enzymes reflect an immediate response to inflammation-mediated destruction of hepatocytes and other hepatic cells. Thus, enzyme elevation is a direct response to hepatic injury. Several hepatic and non-hepatic enzymes leak into the circulation after extensive destruction of hepatocytes and other cells. Such enzymatic elevations are prognostic as well as diagnostic, in that they reflect the degree of chronic liver inflammation due to reactive and unstable chemical species, such as CCl_3 (the metabolic intermediate normally generated from hepatic metabolism of CCl_4). Specifically, elevations in liver enzymes, including AST, ALP, and ALT, directly reflect impaired structural and functional status of the liver. As expected, we observed elevated serum levels of ALP, AST, and ALT, as well as their ratios, in rats in the model group, thus potentially indicating the degree of hepatocyte damage and functional impairment. Interestingly, STRAEZZ-treated rats showed serum levels of hepatic enzymes comparable to those in the control group and lower than those in the model group; these findings suggested that STRAEZZ interferes with chronic inflammation, in a possible mechanism halting hepatocarcinogenesis progression.

The liver, the main metabolizing organ in the body, is equipped with diverse enzyme systems and cell types that enable metabolism of both xenobiotics and endogenous biological molecules. For instance, the liver plays a key role in the reticuloendothelial system for the metabolism of heme from red blood cell breakdown. The reticuloendothelial system breaks down red blood cells (RBCs) and releases the heme moiety into the blood. Heme oxygenase converts the heme moiety into biliverdin, which in turn is converted into bilirubin by biliverdin reductase. Bilirubin forms a complex with albumin, which is then transported to the liver for further biotransformation into inactive and excretable forms. In the liver, hepatocytes aid in recovery of albumin and conjugation of bilirubin with glucuronic acid to form a glucuronide, which is released into the gastrointestinal tract via bile secretion. The fate of bilirubin is determined partly by the resident intestinal microbiota, some of which may hydrolyze glucuronide and consequently lead to absorbable forms of bilirubin returning to the hepatic circulation, in a phenomenon called entero-hepatic recirculation. In the absence of entero-hepatic recirculation, bilirubin is converted into stercobilinogen and urobilinogen for intestinal and renal excretion, respectively. Hypoalbuminemia and hypoproteinemia are associated with chronic hepatic inflammation, liver cirrhosis, and kidney disease.[30] The inability of the liver to produce albumin leads to accumulation of bilirubin in the blood and subsequent toxicity. In this study, the model rats demonstrated high serum levels of direct and indirect bilirubin, reflecting hypoalbuminemia and high hepatocyte necrosis. Unlike the model rats, SRAEZZ-treated rats with an HCC-like phenotype demonstrated lower serum bilirubin levels comparable

those in control rats, thereby indicating the potential of SRAEZZ to induce hepatocyte recovery and improved albumin production by the recovered hepatocytes. The possible recovery of hepatocytes after SRAEZZ treatment manifested as lower AFP levels in SRAEZZ-treated rats with an HCC-like phenotype than in model rats.

Hepatotoxic agents cause extensive derangement in the microarchitecture of the liver. For instance, H&E stained sections of representative livers from the groups showed extensive destruction of the hepatic microstructure of model rats, in contrast to the control rats; this observation correlated with poorer survival rates among the model group than the control group. However, SRAEZZ-treated rats with an HCC-like phenotype demonstrated visible improvement in the hepatic microstructure relative to model rats, as corroborated by improved survival rates.

The bioactivity of plant-derived drugs reflects their secondary plant metabolite composition and the functional group enrichment of the secondary plant metabolites, as well as the amount of each secondary plant metabolite. In this study, chemical characterization of SRAEZZ led to the isolation of two quaternary alkaloids (Q1 and Q2), among which Q1 was without impurities. Further structural elucidation of Q1 led to isolation of quaternary phenanthridin alkaloid. Although the yield of Q1 and Q2 precluded their use in animal studies, the prophylactic anti-HCC effects of SRAEZZ are partly attributable to its quaternary phenanthridin alkaloids. Further chemical investigation of the isolated quaternary phenanthridin alkaloid revealed its chemical relatedness to chelerythrine. Interestingly, chelerythrine, isolated primarily from four medicinal plants—*Zanthoxylum asiaticum* (L.) Appelhans, Groppo & J. Wen; *Chelidonium majus* L.; *Macleaya cordata* (Willd.) R. Br.; and *Sanguinaria canadensis* L.—have demonstrated anti-cancer properties against many cancer subtypes.[16,31,32] *Zanthoxylum asiaticum* L., one of the four medicinal plants from which chelerythrine was isolated, has the same genus as *Z. zanthoxyloides*, the source of quaternary phenanthridin alkaloids, thus suggesting possible phylogenetic relationships with respect to their anti-cancer properties.

The present study might have benefited from using the single isolated quaternary phenanthridin alkaloid (QI) in all bioassays, but its yield was too low to use; nonetheless, it was part of the crude alkaloids and might potentially account for the observed prophylactic anti-HCC effects. In addition, the study might have benefited from docking studies on the isolated quaternary phenanthridin alkaloids to potentially characterize protein−protein interactions and expand understanding of the molecular mechanisms and target binding profiles. Nonetheless, the findings from this study provide a background for further studies on SRAEZZ and Q1, particularly their potential as natural templates for anti-cancer drug development.

Conclusion

SRAEZZ demonstrated prophylactic anti-HCC effects against CCl_4/olive oil-induced HCC-like phenotypes in rats. This finding highlights the potential of alkaloids derived from *Z. zanthoxyloides* to serve as natural templates for developing novel anti-cancer drugs. Additionally, this finding provides a rationale for further studies exploring the optimization of quaternary phenanthridin alkaloid sources and yield for translational studies.

Source of funding

This study was supported by a local research support grant from the Directorate of Research, Innovation and Consultancy (DRIC), University of Cape Coast, Ghana.

Conflict of interest

The authors have no conflict of interest to declare.

Ethical approval

All animal experiments, procedures, and techniques were approved (UCCIRB/EXT/2021/14) by the Institutional Review Board of the University of Cape Coast in 2021. In addition, animal experiments were conducted in complete adherence with the Guidelines of the National Institutes of Health for the care and humane use of animals in scientific experimentation (NIH publication No. 85-23, revised 1985).

Authors contributions

AB: Conceived and designed experiments, wrote the draft manuscript, and reviewed the final manuscript for intellectual content. JKA and VYAB: Carried out crude alkaloid preparation, initial phytochemical screening, isolation of Q1 and Q2, and HPLC and NMR characterization of Q1 and Q2. OM: Performed *in vivo* experiments and analyzed data. EAA: Performed histological experiments and interpreted data. MAE and DD: Performed data analysis and retrieved information. All authors have critically reviewed and approved the final draft and are responsible for the content and similarity index of the manuscript.

Acknowledgment

The authors are grateful to the Directorate of Research, Innovation and Consultancy (DRIC), University of Cape Coast, Ghana, for providing the grant for this research.

Data availability

All data have been provided in the article.

Appendix A. Supplementary data

Supplementary data to this article can be found online at https://doi.org/10.1016/j.jtumed.2024.06.009.

References

1. Sagnelli E, Macera M, Russo A, Coppola N, Sagnelli C. Epidemiological and etiological variations in hepatocellular carcinoma. **Infection 2020**; 48(1): 7−17. https://doi.org/10.1007/s15010-019-01345-y.

2. McGlynn KA, Petrick JL, El-Serag HB. Epidemiology of hepatocellular carcinoma. **Hepatology (Baltimore, Md) 2021**; 73(Suppl 1): 4–13. https://doi.org/10.1002/hep.31288.
3. Vogel A, Meyer T, Sapisochin G, Salem R, Saborowski A. Hepatocellular carcinoma. **Lancet (London, England) 2022**; 400(10360): 1345–1362. https://doi.org/10.1016/s0140-6736(22)01200-4.
4. Zhang CH, Cheng Y, Zhang S, Fan J, Gao Q. Changing epidemiology of hepatocellular carcinoma in Asia. **Liver Int Off J Int Assoc Study Liver 2022**; 42(9): 2029–2041. https://doi.org/10.1111/liv.15251.
5. Yu S, Wang Y, Lv K, Hou J, Li W, Wang X, et al. NT157 inhibits HCC Migration via downregulating the STAT3/Jab1 signaling pathway. **Technol Cancer Res Treat 2021**; 20:15330338211027916. https://doi.org/10.1177/15330338211027916.
6. Rumgay H, Arnold M, Ferlay J, Lesi O, Cabasag CJ, Vignat J, et al. Global burden of primary liver cancer in 2020 and predictions to 2040. **J Hepatol 2022**; 77(6): 1598–1606. https://doi.org/10.1016/j.jhep.2022.08.021.
7. Mbaga DS, Kenmoe S, Kengne-Ndé C, Ebogo-Belobo JT, Mahamat G, Foe-Essomba JR, et al. Hepatitis B, C and D virus infections and risk of hepatocellular carcinoma in Africa: a meta-analysis including sensitivity analyses for studies comparable for confounders. **PLoS One 2022**; 17(1):e0262903. https://doi.org/10.1371/journal.pone.0262903.
8. Seitz HK, Bataller R, Cortez-Pinto H, Gao B, Gual A, Lackner C, et al. Alcoholic liver disease. **Nat Rev Dis Prim 2018**; 4(1): 16. https://doi.org/10.1038/s41572-018-0014-7.
9. Zhang X, Coker OO, Chu ES, Fu K, Lau HCH, Wang YX, et al. Dietary cholesterol drives fatty liver-associated liver cancer by modulating gut microbiota and metabolites. **Gut 2021**; 70(4): 761–774. https://doi.org/10.1136/gutjnl-2019-319664.
10. Groopman JD, Smith JW, Rivera-Andrade A, Alvarez CS, Kroker-Lobos MF, Egner PA, et al. Aflatoxin and the etiology of liver cancer and its implications for Guatemala. **World Mycotoxin J 2021**; 14(3): 305–317. https://doi.org/10.3920/wmj2020.2641.
11. Badraoui R, Siddiqui AJ, Bardakci F, Ben-Nasr H. Ethnopharmacology and ethnopharmacognosy - current perspectives and future prospects. In: *Ethnobotany and ethnopharmacology of medicinal and aromatic plants*. Taylor & Francis; 2023. pp. 1–14.
12. Bédoui I, Nasr HB, Ksouda K, Ayadi W, Louati N, Chamkha M, et al. Phytochemical composition, bioavailability and pharmacokinetics of scorzonera undulata methanolic extracts: antioxidant, anticancer, and apoptotic effects on MCF7 cells. **Phcog Mag 2024**; 20(1): 218–229. https://doi.org/10.1177/09731296231207231.
13. Reddy B, Fan AY. Incorporation of complementary and traditional medicine in ICD-11. **BMC Med Inf Decis Making 2022**; 21(Suppl 6): 381. https://doi.org/10.1186/s12911-022-01913-7.
14. Fu YH, Guo JM, Xie YT, Hua J, Dai YY, Zhang W, et al. Structural characterization, antiproliferative and anti-inflammatory activities of alkaloids from the roots of Zanthoxylum austrosinense. **Bioorg Chem 2020**; 102:104101. https://doi.org/10.1016/j.bioorg.2020.104101.
15. Acheampong DO, Baffour IK, Atsu Barku VY, Addo JK, Essuman MA, Boye A. Zanthoxylum zanthoxyloides alkaloidal extract improves CCl(4)-induced hepatocellular carcinoma-like phenotypes in rats. **Evid Base Compl Alternative Med eCAM 2021**; 2021:3804379. https://doi.org/10.1155/2021/3804379.
16. Chen N, Qi Y, Ma X, Xiao X, Liu Q, Xia T, et al. Rediscovery of traditional plant medicine: an underestimated anticancer drug of chelerythrine. **Front Pharmacol 2022**; 13:906301. https://doi.org/10.3389/fphar.2022.906301.
17. Basu A, Kumar GS. Interaction of the putative anticancer alkaloid chelerythrine with nucleic acids: biophysical perspectives. **Biophys Rev 2020**; 12(6): 1369–1386. https://doi.org/10.1007/s12551-020-00769-3.
18. Qu L, Liang X, Tian G, Zhang G, Wu Q, Huang X, et al. Efficacy and safety of mulberry twig alkaloids tablet for the treatment of type 2 diabetes: a multicenter, randomized, double-blind, double-dummy, and parallel controlled clinical trial. **Diabetes Care 2021**; 44(6): 1324–1333. https://doi.org/10.2337/dc20-2109.
19. Ben Mosbah I, Massip-Salcedo M, Fernández-Monteiro I, Xaus C, Bartrons R, Boillot O, et al. Addition of adenosine monophosphate-activated protein kinase activators to University of Wisconsin solution: a way of protecting rat steatotic livers. **Liver Transplant 2007**; 13(3): 410–425.
20. Lin J, Dai Y, Sang C, Song G, Xiang B, Zhang M, et al. Multimodule characterization of immune subgroups in intrahepatic cholangiocarcinoma reveals distinct therapeutic vulnerabilities. **J Immunother Cancer 2022**; 10(7). https://doi.org/10.1136/jitc-2022-004892.
21. El-Sheekh MM, Nassef M, Bases E, Shafay SE, El-Shenody R. Antitumor immunity and therapeutic properties of marine seaweeds-derived extracts in the treatment of cancer. **Cancer Cell Int 2022**; 22(1): 267. https://doi.org/10.1186/s12935-022-02683-y.
22. Jiang M, Huang C, Wu Q, Su Y, Wang X, Xuan Z, et al. Sini San ameliorates CCl4-induced liver fibrosis in mice by inhibiting AKT-mediated hepatocyte apoptosis. **J Ethnopharmacol 2023**; 303:115965. https://doi.org/10.1016/j.jep.2022.115965.
23. Wang M, Lan L, Yang F, Jiang S, Xu H, Zhang C, et al. Hepatic SIRT6 deficit promotes liver tumorigenesis in the mice models. **Genes & diseases 2022**; 9(3): 789–796. https://doi.org/10.1016/j.gendis.2020.08.007.
24. Unsal V, Cicek M, Sabancilar İ. Toxicity of carbon tetrachloride, free radicals and role of antioxidants. **Rev Environ Health 2021**; 36(2): 279–295. https://doi.org/10.1515/reveh-2020-0048.
25. Rahmouni F, Saoudi M, Amri N, El-Feki A, Rebai T, Badraoui R. Protective effect of Teucrium polium on carbon tetrachloride induced genotoxicity and oxidative stress in rats. **Arch Physiol Biochem 2018**; 124(1): 1–9. https://doi.org/10.1080/13813455.2017.1347795.
26. Rahmouni F, Hamdaoui L, Badraoui R, Rebai T. Protective effects of Teucrium polium aqueous extract and ascorbic acid on hematological and some biochemical parameters against carbon tetrachloride (CCl4) induced toxicity in rats. **Biomed Pharmacother 2017**; 91: 43–48. https://doi.org/10.1016/j.biopha.2017.04.071.
27. Rahmouni F, Badraoui R, Ben-Nasr H, Bardakci F, Elkahoui S, Siddiqui AJ, et al. Pharmacokinetics and therapeutic potential of Teucrium polium against liver damage associated hepatotoxicity and oxidative injury in rats: computational, biochemical and histological studies. **Life 2022**; 12(7). https://doi.org/10.3390/life12071092.
28. Linson EA, Hanauer SB. More than a tumor marker…A potential role for alpha-feto protein in inflammatory bowel disease. **Inflamm Bowel Dis 2019**; 25(7): 1271–1276. https://doi.org/10.1093/ibd/izy394.
29. Alami F, Alizadeh M, Shateri K. The effect of a fruit-rich diet on liver biomarkers, insulin resistance, and lipid profile in patients with non-alcoholic fatty liver disease: a randomized clinical trial. **Scand J Gastroenterol 2022**; 57(10): 1238–1249. https://doi.org/10.1080/00365521.2022.2071109.
30. Yoshida S, Fujita M, Ishigame T, Kobayashi Y, Sumichika Y, Saito K, et al. Case report: unusual development of hepatocellular carcinoma during immunosuppressive treatments against rheumatoid arthritis overlapping Sjögren's syndrome; cirrhotic steatohepatitis with liver inflammation and fibrosis lurks in autoimmune disorders. **Front Immunol 2023**; 14: 1089492. https://doi.org/10.3389/fimmu.2023.1089492.

31. Wu S, Yang Y, Li F, Huang L, Han Z, Wang G, et al. Chelerythrine induced cell death through ROS-dependent ER stress in human prostate cancer cells. **OncoTargets Ther 2018**; 11: 2593–2601. https://doi.org/10.2147/ott.s157707.
32. Cho O, Lee JW, Kim HS, Jeong YJ, Heo TH. Chelerythrine, a novel small molecule targeting IL-2, inhibits melanoma progression by blocking the interaction between IL-2 and its receptor. **Life Sci 2023**; 320:121559. https://doi.org/10.1016/j.lfs.2023.121559.

How to cite this article: Boye A, Barku VA, Addo JK, Martey O, Asiamah EA, Essuman MA, Doe D. *Zanthoxylum zanthoxyloides* (Lam.) B. Zepernick & Timler alkaloidal extract exerts hepatoprotective effects in rats with a CCl_4/olive oil-induced hepatocellular carcinoma-like phenotype. J Taibah Univ Med Sc 2024;19(4):753–765.